Generation of high-order spatially coherent harmonics from solid targets by femtosecond laser pulses

A. Tarasevitch, A. Orisch, and D. von der Linde
Institut für Laser- und Plasmaphysik, Universität-GHS-Essen, D-45117 Essen, Germany

Ph. Balcou, G. Rey, and J.-P. Chambaret
Laboratoire d'Optique Appliquée, ENSTA-Ecole Polytechnique, 91761 Palaiseau, France

U. Teubner, D. Klöpfel, and W. Theobald
Institut für Optik und Quantenelektronik, Friedrich-Schiller-Universität Jena, Max-Wien-Platz 1, 07743 Jena, Germany
(Received 20 January 2000; published 20 July 2000)

This paper discusses the generation of high-order optical harmonics from solid targets using laser pulses of 35 and 120 femtoseconds. Harmonics up to the 35th order were observed. High conversion efficiency has been achieved, e.g., 10^{-6} to the 10th harmonic. It is demonstrated that the harmonic emission is highly directional and that the harmonic efficiency decreases rapidly with increasing plasma scale length.

PACS number(s): 42.65.Ky, 52.40.Nk, 52.50.Jm

I. INTRODUCTION

Generation of optical harmonics of high order is one of the most promising tools for generating short wavelength coherent radiation. In noble gases harmonics up to about the 300th order have been produced [1,2]. A different approach is high-order harmonic generation (HOHG) in reflection from solid targets. The mechanism of the latter type HOHG can be qualitatively explained using the simple physical model of an oscillating plasma mirror [3–6]. Indeed, the target surface is highly ionized by the leading edge of the pump pulse, and a reflecting layer of supercritical plasma is formed. When the details of the electron density distribution are neglected, the collective electron motion created by the incident electromagnetic wave can be considered as an oscillating mirror. The phase modulation of the reflected light introduced by this mirror gives rise to harmonic frequencies. The descriptive ''mirror model'' and detailed particle-in-cell (PIC) simulations show that at relativistic intensities ($I \geqslant 10^{18}$ W/cm^2) the number of harmonics and the conversion efficiency are strongly enhanced [3–7]. The use of rapidly developing femtosecond laser systems capable of producing strong light pulses in the relativistic intensity regime presents interesting new possibilities.

Harmonic generation from solid targets is still much less developed than HOHG in gases. First, it requires much higher laser intensities. For harmonic generation in gaseous media the laser intensity is limited by the onset of ionization of the atoms, which occurs at intensities less than 10^{16} W/cm^2. Secondly, a steplike plasma-vacuum interface is essential for HOHG in reflection. In the first experiments with nanosecond CO_2 lasers [8] and in experiments by Norreys *et al.* with picosecond pulses [9] the pulse duration was long enough for the plasma to expand considerably into the vacuum during the pulse. In these cases HOHG was explained by the steepening of the plasma-vacuum interface due to strong ponderomotive forces. However, the harmonic radiation in the picosecond experiments [9,10] showed substantial spectral broadening and a very wide angular distribution, not expected for the generation of reflected harmonics from a planar interface. These observations were attributed to the self-phase modulation in the tail of underdense plasma and rippling of the plasma surface [10].

The use of femtosecond pump pulses leads quite naturally to the formation of a steep gradient of the plasma density because there is no time for significant plasma expansion during the pulse duration. Moreover, after creating a plasma with a femtosecond pulse, one can let the plasma expand for a certain amount of time to establish a plasma scale length of any desired value. Using a second, time-delayed femtosecond pulse for the generation of the harmonics, one can explicitly investigate the influence of the plasma scale length on the HOHG.

An important point of HOHG from solid targets is the fact that laser pulses of very high contrast are required. A prepulse or a slowly rising leading front of the pump pulse lead to premature ionization of the target and destruction of the steep density profile long before the arrival of the high-intensity pulse maximum.

Experimentally, using pulses of approximately 100 fs from titanium sapphire lasers operating in the chirped pulse amplification (CPA) mode, harmonics up to the 7th order have been observed by Kohlweyer *et al.* [11], up to 16th order by Zepf *et al.* [12], and up to 18th by von der Linde *et al.* [13]. The importance of a clean rising edge of the laser pulses in HOHG was demonstrated in Ref. [12]. So far, however, the direct observations of the influence of the plasma scale length on harmonic efficiency, as well as detailed measurements of the angular distribution demonstrating the directionality of the harmonics, are still lacking.

In this paper we wish to report on the results of a series of HOHG experiments in which high contrast ratio laser pulses up to relativistic intensities were used. The aim of this work was (i) to extend HOHG from solid targets to higher orders, (ii) to determine the divergence of the harmonics, and (iii) to carry out direct measurements of the influence of the plasma scale length on HOHG.

II. EXPERIMENTAL

A schematic of the experimental setup is shown in Fig. 1. The incident laser pulses at the wavelength of 800 nm were

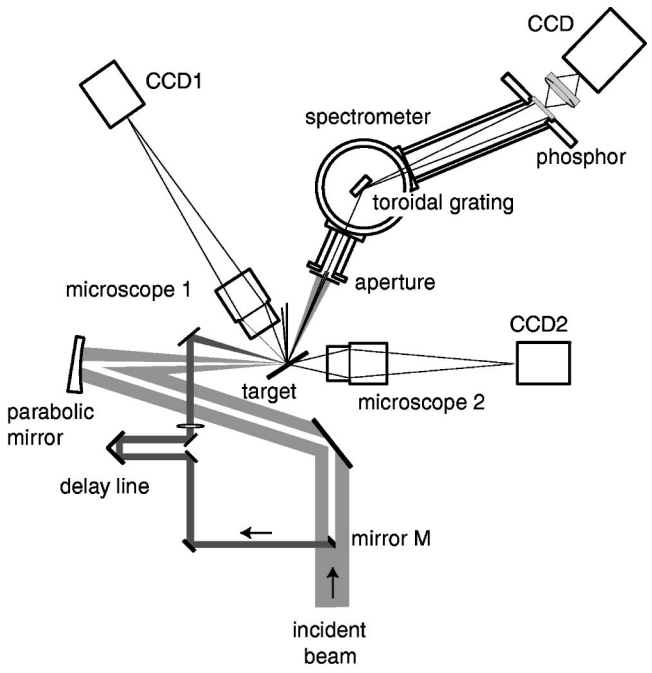

FIG. 1. Schematic of the experimental setup.

focused onto the target with the help of an off-axis parabolic mirror. The spectrum of the reflected light was imaged onto a phosphor screen with the help of a toroidal grating, and the phosphorescent light was recorded with a CCD camera.

A small mirror *M* was placed in the incident laser beam to block the center and to reflect a small portion of the incident laser pulse into a second channel with a variable optical path length. This mirror served two purposes. First, with the second channel a pair of laser pulses with variable time delay was available for pump-probe experiments. Secondly, the mirror prevented reflected laser light from the target from entering the spectrometer [14]. The position of the mirror was chosen so that the parabolic mirror produced an image of *M* on the entrance aperture of the spectrometer. The diameter of the aperture was suitably adjusted to completely block the specularly reflected laser light. On the other hand, harmonic radiation propagating on axis, close to the specular direction, passed through the hole of the aperture into the spectrometer.

Several long focal length, aberration-corrected objective lenses were used in conjunction with CCD cameras for precise alignment of the target, the object point of the toroidal grating, and the laser focal point. A positioning accuracy of 2 μm along three orthogonal axes was achieved. The alignment was continuously monitored during the experiments with the help of the objective lenses and cameras.

The targets were optically polished glass substrates, which were raster scanned to provide a fresh surface for each laser pulse. The pressure in the experimental chamber was 10^{-3} Torr.

III. RESULTS

A. Experiments with pulses of 35 fs

In a first series of experiments, a titanium sapphire laser system [15] with pulses of 35 fs and pulse energy up to 50 mJ was used. The laser intensity on the target reached $5\times10^{17}-10^{18}$ W/cm^2. The incident laser pulses were *p* polarized at an angle of incidence of 55°. The ratio of the laser intensity at 1 ps before the peak and the peak intensity (contrast ratio) was approximately 10^{-6}.

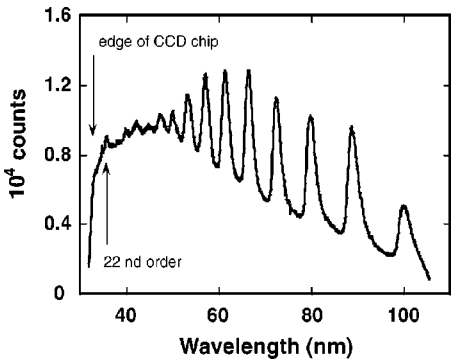

FIG. 2. Long wavelength side of the harmonic spectrum. The spectrum is averaged over 70 laser pulses. Pulse duration: 35 fs; laser intensity: 5×10^{17} W/cm^2.

Examples of typical harmonic spectra [6] are depicted in Figs. 2 and 3. The spectra were integrated over 70 pulses. In the long wavelength region (Fig. 2) even and odd harmonics were observed from the 8th to the 22nd order. The harmonics are superimposed on some background, which is probably due to incoherent emission from the plasma. In Fig. 2 the spatial dimensions of the CCD chip limited the wavelength range of the spectrum.

Figure 3 shows an example of the short wavelength region of the harmonic spectra. In this case, the reflected light was passed through a 150 nm thick aluminum foil to suppress the emission at longer wavelengths. The spectrum is corrected for the transmission curve of the Al filter.

The sharp cutoff at the short wavelength side corresponds to the *L*-absorption edge of aluminum at approximately 18 nm. As in Fig. 2, the harmonic spectrum has a strong background. Nevertheless, one can clearly trace peaks coinciding with the positions of harmonics up to 45th order. Unfortunately, a series of oxygen ion line appears in the range 18 to 21 nm. Because the oxygen ion lines tend to obscure the harmonic spectrum, an unambiguous identification of the harmonic peaks is possible only up to the 35th order. Nevertheless, our results represent the highest harmonic orders

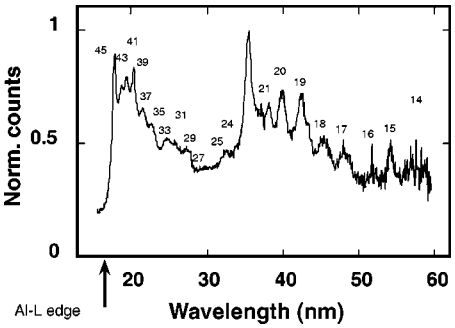

FIG. 3. Short wavelength side of the harmonic spectrum. Other parameters are same as in Fig. 2.

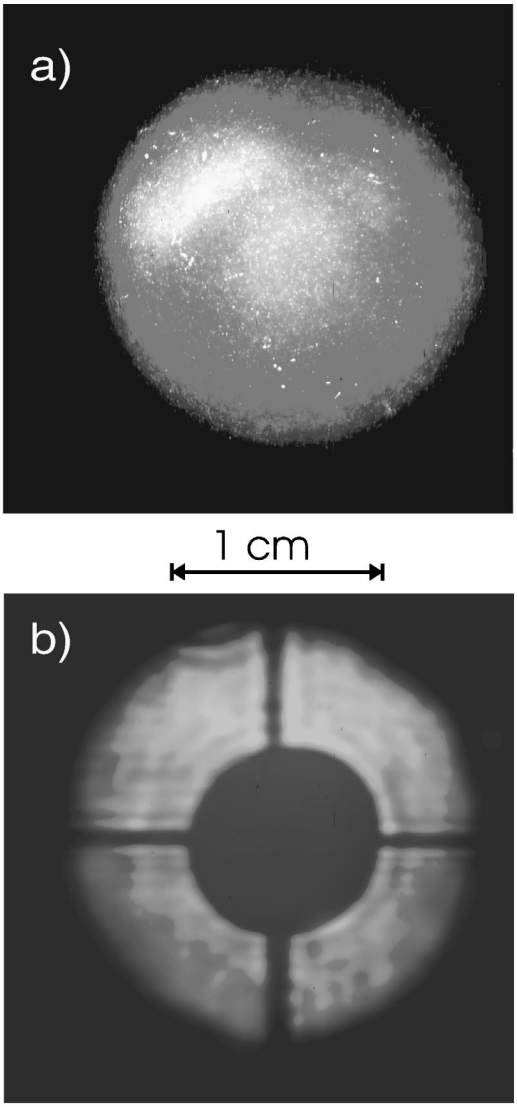

FIG. 4. Spatial distribution of the radiation from the target recorded on a phosphor screen. The distance from the target is about 10 cm. (a) Reflected fundamental blocked with filters; (b) distribution of the fundamental.

observed to date for femtosecond HOHG from solid targets. It is interesting to note that starting from 23rd to 25th order odd harmonics are slightly stronger than even ones.

The origin of the peak near 35–40 nm (position of harmonics 22–20) is not quite clear as yet. One of the possible explanations of this line is emission at $2\omega_p$ due to the excitation of plasma waves by hot electrons, as discussed in Ref. [16]. Alternatively, the peak near 35–40 nm could be due to a resonance of the harmonics around 20th–22nd order with plasma oscillations.

A qualitative observation of angular divergence of the harmonic radiation was made as follows. We let the reflected beam from the target directly strike a phosphor screen and recorded the spatial distribution of the phosphorescence with a CCD camera. The fundamental radiation scattered from the screen was blocked with suitable optical filters. Figure 4(a) shows the distribution of the phosphorescence generated by

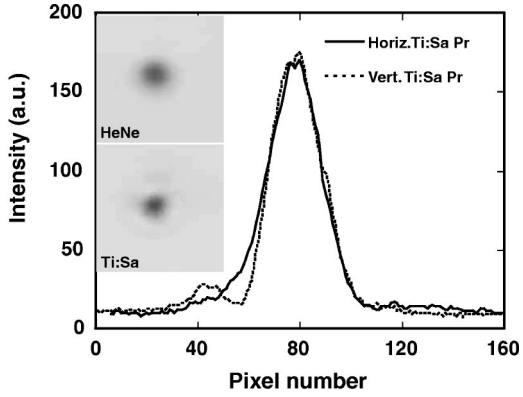

FIG. 5. Far field spatial distribution of the 120 fs titanium sapphire laser.

the short wavelength radiation. The image is of course integrated over all orders of harmonics. Figure 4(a) shows that the beam of the harmonics is highly directional and nearly spatially uniform. From the observed distribution we estimate the angular divergence of the integrated harmonic beam to be 50 to 100 mrad, somewhat narrower than the focused fundamental, which has an angular width of approximately 100 mrad.

Care had to be exercised in order to distinguish phosphorescence produced by harmonic radiation from two-photon-excited phosphorescence generated by the intense fundamental laser beam. Figure 4(b) shows an image of the cross section of the fundamental laser beam recorded by two-photon phosphorescence. Note that two-photon recording is expected to strongly enhance inhomogeneities in the fundamental beam.

The black disk in the center and the orthogonal thin black lines represent the image of the beam splitting mirror M (see Fig. 1) and the supporting wires, respectively. This structure is characteristic of the fundamental beam. Comparison with Fig. 4(a) shows that the features due to the splitting mirror and its support are absent at the harmonic frequencies, as expected. Thus the spatial distributions of the fundamental and the harmonics can be easily distinguished.

Completely different angular distributions were observed when the pump intensity exceeded 10^{18} W/cm^2. The reflected light was no longer collimated, but spread over a large solid angle around the specular direction. No harmonic radiation could be detected on top of the incoherent plasma emission, which became much stronger as the laser intensity was increased. It should be mentioned that we were unable to detect harmonics with *s*-polarized laser pulses.

B. Experiments with pulses of 120 fs

In the different series of experiments we used a titanium sapphire system with a pulse duration of 120 fs and an energy up to 70 mJ. The contrast ratio was better than 10^{-4} at 1 ps from the pulse maximum. Important for the following experiments were very good spatial beam quality and a high pulse stability.

Figure 5 shows the far field spatial intensity distribution

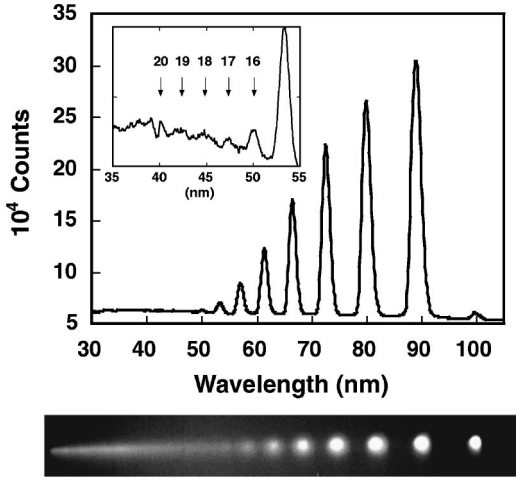

FIG. 6. Harmonic spectrum recorded with 120 fs pulses and at 2×10^{17} W/cm^2. The actual image of the output plane of the spectrometer is shown below.

of the titanium sapphire laser beam. The corresponding distribution of the He-Ne alignment laser is also shown for comparison. Using an off-axis parabolic mirror with a 10 cm focal length for focusing, a spot diameter of 12 μm was obtained in the focal plane.

An example of harmonic spectrum recorded with this laser is depicted in Fig. 6. The spectrum is an integral over 100 laser pulses. The background is much lower than in the previous experiments. The insert shows that harmonics up to the 20th order could be distinguished. The actual image of the output plane of the spectrometer is also shown. Note that the spots corresponding to different harmonic orders are perfectly circular, indicating an excellent beam quality and good imaging properties of the toroidal grating.

1. Measurements of harmonic divergence and efficiency

In order to study the angular divergence, the harmonic beams were scanned across the entrance aperture of the spectrometer by rotating the sample (see Fig. 7). The aperture corresponded to an acceptance angle of 0.5°. With the help of the set of the objective lenses (Fig. 1) the position of the sample was carefully controlled in order to avoid a misalignment of the system when the target angle was changed.

The full divergence angle of the fundamental radiation was measured to be 7.3°. The measured angular dependence

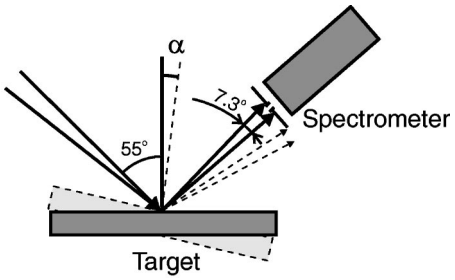

FIG. 7. Schematic of the measurement of the divergence of high order harmonics. The aperture in front of the spectrometer corresponds to the acceptance angle of 0.5°.

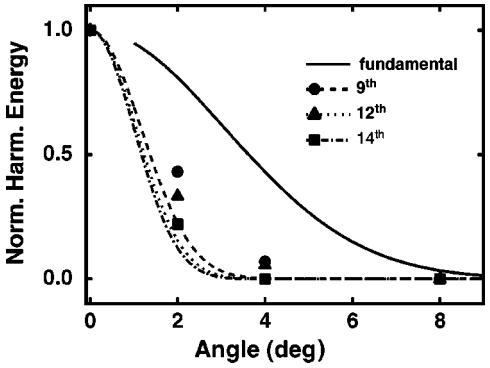

FIG. 8. Angular distribution of the 9th, 12th, 14th harmonic, and of the reflected fundamental. Dashed, dotted and dash-dotted lines represent the calculated distribution for the 9th, 12th, and 14th harmonics, respectively.

of the harmonic energy is shown in Fig. 8 together with the angular distribution of the reflected fundamental for comparison. The center of the fundamental beam blocked by the beam splitting mirror is disregarded in Fig. 8.

It is clear that the divergence of the harmonics is smaller than that of the fundamental. If, for the purpose of comparison, we assume a power law for the harmonic intensity and a Gaussian beam profile, the divergence angle of the nth harmonic $\Delta\Theta_n$ should scale as $\Delta\Theta/\sqrt{n}$, where $\Delta\Theta$ is the divergence angle of the fundamental. The corresponding angular distributions are also plotted in Fig. 8. Comparing the experimental data with these curves, we conclude that the emitted harmonics are nearly diffraction limited or, in other words, highly spatially coherent.

The conversion efficiency η_n of HOHG can be estimated using the expression

$$\eta_n=\frac{E_n}{E_F}=\frac{\Omega_n K_{\mathrm{gr}}\hbar\omega n_e}{E_F\Omega_0\eta_{\mathrm{ph}}\eta_{\mathrm{CCD}}},$$

where E_n and E_F are the energies of the nth harmonic and the fundamental, Ω_n and Ω_0 denote the solid angles of the harmonic beam and of the spectrometer acceptance, K_{gr} is the attenuation of harmonic signal due to the grating, $\hbar\omega$ is the photon energy, η_{ph} and η_{CCD} are the conversion efficiency of the phosphor screen and the quantum yield of the CCD camera [17], respectively, and n_e is the number of the photoelectrons recorded by the CCD camera.

K_{gr} as a function of the wavelength was taken from data provided by the grating manufacturer. To determine the η_{ph} we have made a series of calibration measurements using a hollow cathode lamp [18] with and without phosphor screen. Using the formula given above we obtain an efficiency of 10^{-7} for the 10th and 10^{-8} for the 15th harmonic. The corresponding estimates for the experiments carried out with the 35 fs laser system are 10^{-6} and 10^{-7} for the 10th and 15th harmonic, respectively.

According to our estimate, the efficiencies observed on solid targets are comparable with those of HOHG in noble gases. For example, in Ref. [19] the conversion efficiency for the 5th to 23rd harmonic in Xe was estimated to be approxi-

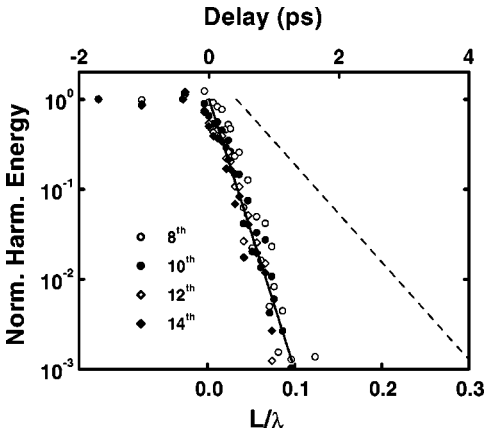

FIG. 9. Energy of different harmonics as a function of the time delay (upper horizontal scale). Lower horizontal scale: Estimated plasma scale length. Solid line: $\exp(-L/0.015\lambda)$. Dashed line: Dependence of the harmonic energy on the scale length calculated in Ref. [12].

mately 10^{-6}. This would correspond to the efficiency of the 10th harmonic in our experiments with pulses of 35 fs. The comparison of the efficiency of HOHG from solid targets and from gas targets is clearly somewhat arbitrary, because of the very different high frequency roll-off in the two cases.

Estimates of the conversion efficiency can be subject to systematic errors. For example, in our estimate we have used the grating efficiency data given by the manufacturer. Our own measurements at several selected wavelengths show a factor of 2 lower diffraction efficiency of the toroidal grating. This discrepancy could be due to contamination of the grating surface. Also, differences between the actual value of η_{CCD} of our CCD camera and the published values cannot be excluded. Another source of potential error is the estimation of the solid angle $\Omega_n \approx \pi(\Delta\Theta_n)^2$ for which we assume an accuracy of about $\pm 25\%$. Taking into account these possible sources of error, the conversion efficiencies η_n given here are probably subject to an uncertainty of a factor of 3 to 4.

2. Dependence of the harmonic efficiency on plasma scale length

Pump-probe experiments were carried out in order to investigate the dependence of HOHG efficiency on the plasma scale length. These measurements were performed with the 120 fs titanium sapphire laser system. A plasma was created on the surface of the target by a first, relatively weak laser pulse (5×10^{14} W/cm^2). A second pulse with an adjustable time delay τ with respect to the first pulse was used to produce harmonics. The intensity of the second pulse was approximately 2×10^{17} W/cm^2.

The measured dependence of the harmonic energy on τ for several harmonic orders is depicted in Fig. 9. The available dynamic range of our measurements was 10^3. For all harmonic orders the energies decrease rapidly, and the decay of the harmonic signals is approximately the same. The data can be fitted by an exponential function, $\exp(-\tau/\tau_s)$, with $\tau_s = 200$ fs.

The experimental data in Fig. 9 were obtained in two successive series of measurements. The results demonstrate a low spread of the experimental data, indicating excellent reproducibility of the harmonic signals and good stability of the laser parameters.

For an interpretation of the observed decay of harmonic generation with delay time we used a simple isothermal model of plasma expansion [20]. The spatial profile of the electron density is taken to be $N_e = N_0 \exp(-z/L)$. Here, L is the plasma scale length which grows according to $L = v_T\tau$, where $v_T = \sqrt{ZkT_e/M}$ is the expansion velocity of the plasma. T_e is the electron temperature, Z is the ionization degree, k is the Boltzmann constant, and M is the ion mass.

For the pulse energy used in the experiment to create the plasma (first laser pulse) we estimated the electron temperature T_e and the expansion velocity v_T to be 100 eV and 6×10^6 cm/s, respectively. We used the value $v_T = 6\times10^6$ cm/s $= 0.075\ \lambda$/ps to convert experimental delay time to plasma density scale length. These values agree well with the results obtained from spectral interferometry of the light reflected from the plasma [21], and from measurements of the Doppler shift and of the plasma reflectivity [22]. With these numbers the solid line in Fig. 9 falls off as $\exp(-L/L_s)$ with $L_s = 0.015\lambda$.

Our data show that the decrease of harmonic generation with scale length is quite fast in comparison with available PIC simulations. The dashed line in Fig. 9 shows the calculated dependence of the harmonic efficiency on scale length form a recent PIC simulation [4,12]. Another important qualitative difference is that in our experiments the harmonic efficiency decreases monotonically with the plasma scale length. An ''optimum'' scale length for the HOHG as predicted in Ref. [23] was not observed. We note, however, that this comparison must be regarded with caution, because physical parameters of the calculation do not correspond to our experimental situation. Furthermore, the simulations were performed with a fixed linear density profile, and a possible deformation of the profile due to ponderomotive forces was not taken into account.

IV. CONCLUSIONS

In conclusion, we have reported the highest harmonic order observed to date in femtosecond harmonic generation from solid targets. High conversion efficiency, comparable with that of HOHG in noble gases [19] has been achieved. It has been demonstrated that high-order harmonic emission from solid targets is nearly diffraction limited. Laser pulses with high contrast ratio and steep leading edges and peak intensities not exceeding 10^{18} W/cm^2 are essential for spatially coherent HOHG.

At higher laser intensities we observe a spreading of the reflected fundamental laser radiation and of the harmonic emission over a large solid angle. This observation suggests a deformation of the reflecting plasma surface at very high laser intensity. One might expect that the effect could be avoided with the use of shorter laser pulse. However, the comparison of our experiments with laser pulses of nominally 35 and 120 fs did not indicate any significant difference of the high intensity behavior.

We do not observe a certain optimum scale length for

HOHG during the expansion of the plasma, apparently in contradiction with PIC simulations [4,12]. Also, our experiments show that the efficiency of HOHG drops more rapidly with increasing plasma scale length than predicted by these simulations.

For a possible explanation of the faster decrease the spreading of the harmonic emission at higher intensities is invoked. In our experiments we measured the specular component of harmonic radiation in a relatively narrow solid angle. To produce a drop of 10^3, corresponding to the measured value, it would be sufficient to spread the initially collimated harmonics over a much larger solid angle. Formation of a distortion of the plasma surface in a time of approximately one picosecond, resulting in such a spreading, could explain our observations. Plasma surface distortions, which cannot be taken into account in one-dimensional PIC calculations, could be caused by plasma instabilities, predicted to occur at high laser intensity.

Because a substantial increase of the efficiency of harmonic generation is expected for laser intensities exceeding 10^{18} W/cm^2, it is a great challenge to overcome the present limits. The realization of this potential requires a thorough understanding of the distortion effects. The threshold of the plasma instabilities should strongly depend on the plasma scale length. Therefore, more detailed pump-probe experiments with the diagnostics of plasma surface and of the spatial and angular distribution of the harmonic are important.

ACKNOWLEDGMENTS

The authors gratefully acknowledge experimental contributions from Dr. G. Jenke, theoretical advice from Professor V. P. Silin, and fruitful discussions with Professor A. M. Zheltikov. This work was partially funded by the European Union in the framework of ''Training and Mobility by Research,'' and by the ''International Association for the Promotion of Cooperation with Scientists from the former Soviet Union'' (INTAS). Sustained national financial support by the Deutsche Forschungsgemeinschaft is also gratefully acknowledged.

[1] Z. Chang, A. Rundquist, H. Wang, M.M. Murnane, and H.C. Kapteyn, Phys. Rev. Lett. **79**, 2967 (1997).

[2] Ch. Spielmann, N.H. Burnett, S. Sartania, R. Koppitsch, M. Schnürer, C. Kan, M. Lenzner, P. Wobrauschek, and F. Krausz, Science **278**, 661 (1997).

[3] R. Lichters, J. Meyer-ter-Vehn, and A. Pukhov, Phys. Plasmas **3**, 3425 (1996).

[4] R. Lichters, J. Meyer-ter-Vehn, Inst. Phys. Conf. Ser. **154**, 221 (1997).

[5] D. von der Linde and K. Rzazewski, Appl. Phys. B: Photophys. Laser Chem. **63**, 499 (1996).

[6] D. von der Linde, Appl. Phys. B: Photophys. Laser Chem. **68**, 1 (1999).

[7] P. Gibbon, Phys. Rev. Lett. **76**, 50 (1996).

[8] R.L. Carman, C.K. Rhodes, and R.F. Benjamin, Phys. Rev. A **24**, 2649 (1981).

[9] P.A. Norreys, M. Zepf, S. Moustaizis, A.P. Fews, J. Zhang, P. Lee, M. Bakarezos, C.N. Danson, A. Dyson, P. Gibbon, P. Loukakos, D. Neely, F.N. Walsh, J.S. Wark, and A.E. Dangor, Phys. Rev. Lett. **76**, 1832 (1996).

[10] J. Zhang, M. Zepf, P.A. Norreys, A.E. Dangor, M. Bakarezos, C.N. Danson, A. Dyson, A.P. Fews, P. Gibbon, M.H. Key, P. Lee, P. Loukakos, S. Moustaizis, D. Neely, F.N. Walsh, and J.S. Wark, Phys. Rev. A **54**, 1597 (1996).

[11] S. Kohlweyer, G.D. Tsakiris, C.G. Wahlstrom, C. Tillman, and I. Mercer, Opt. Commun. **117**, 431 (1995).

[12] M. Zepf, G.D. Tsakiris, G. Pretzler, I. Watts, D.M. Chambers, P.A. Norreys, U. Andiel, A.E. Dangor, K. Eidmann, C. Gahn, A. Machacek, J.S. Wark, and K. Witte, Phys. Rev. E **58**, R5253 (1998).

[13] D. von der Linde, T. Engers, G. Jenke, P. Agostini, G. Grillon, E. Nibbering, A. Mysyrowicz, and A. Antonetti, Phys. Rev. A **52**, R25 (1995).

[14] J. Peatross, J.L. Chaloupka, and D.D. Meyerhofer, Opt. Lett. **19**, 942 (1994).

[15] A. Antonetti, F. Blasco, J.P. Chambaret, G. Cheriaux, G. Darpentigny, C. Le Blanc, P. Rousseau, S. Ranc, G. Rey, and F. Salin, Appl. Phys. B: Photophys. Laser Chem. **65**, 197 (1997).

[16] U. Teubner, D. Altenbernd, P. Gibbon, E. Förster, A. Mysyrowicz, P. Audebert, J.-P. Geindre, J.-C. Gauthier, R. Lichters, and J. Meyer-ter-Vehn, Opt. Commun. **144**, 217 (1997); R. Lichters, J. Meyer-ter-Vehn, and A. Pukhov, in *Superstrong Fields in Plasmas*, edited by M. Lontano, G. Monton, F. Pegoraro, and E. Sindoni AIP Conf. Proc. No. 426 (AIP, Woodbury, NY, 1998), p. 41; U. Teubner, P. Gibbon, D. Altenbernd, D. Oberschmidt, E. Förster, A. Mysyrowicz , P. Audebert, J.-P. Geindre, and J.-C. Gauthier, Laser Part. Beams (to be published).

[17] Y. Li, G.D. Tsakiris, and R. Sigel, Rev. Sci. Instrum. **66**, 80 (1995).

[18] K. Danzmann, M. Günter, I. Fischer, M. Kock, and M. Kühne, Appl. Opt. **27**, 4947 (1988).

[19] A. L'Huillier and Ph. Balcou, Phys. Rev. Lett. **70**, 774 (1998).

[20] W. L. Kruer, *The Physics of Laser Plasma Interaction* (Addison-Wessly, Redwood City, CA, 1988).

[21] J.-C. Gauthier, J.P. Geindre, P. Audebert, S. Bastiani, C. Quoix, G. Grillon, A. Mysyrowicz, and R.C. Mancini, Phys. Plasmas **4**, 1811 (1997).

[22] R.V. Volkov, V.M. Gordienko, S.A. Magnitskii, P.G. Oganian, P.A. Oleinikov, V.T. Platonenko, and A.P. Tarasevitch, Quantum Electron. **25**, 877 (1995).

[23] In Ref. [4,12] the linear density ramp is considered. In order to compare the simulations with our density profile we divide the calculated in Ref. [4,12] scale length by the factor of $\ln(N_0/N_c)$. In that case the critical density is reached at the same distance for both profiles linear and exponential. We assume $N_0/N_c \approx 400$ and therefore $\ln(N_0/N_c)=6$.